Micelle gel formation in poly(ethylene oxide)-poly(propylene oxide)-poly(ethylene oxide) triblock copolymer in water solution. Dynamic and static light scattering and oscillatory s...

ARTICLE *in* THE JOURNAL OF PHYSICAL CHEMISTRY · FEBRUARY 1991

Impact Factor: 2.78 · DOI: 10.1021/j100157a064

between the diffusion coefficient data reported by two research groups.[5,8] We could not obtain evidence for such secondary aggregation in CHAPS.

Thus, GFC can provide very accurate C_1 values for CHAPS, which make possible the determination of aggregation numbers and stepwise aggregation constants. These results will be helpful for applications of CHAPS in membrane biochemistry. Furthermore, the present approach can be used for other compounds, such as bile salts, drugs, nucleosides, and dyes.[5-13] The odd-even alternation observed in the aggregation number dependence of stepwise aggregation constants is a novel phenomenon, which has been revealed by the determination of very accurate V_c values.

Micelle and Gel Formation in a Poly(ethylene oxide)/Poly(propylene oxide)/Poly(ethylene oxide) Triblock Copolymer in Water Solution. Dynamic and Static Light Scattering and Oscillatory Shear Measurements

Wyn Brown,* Karin Schillén, Mats Almgren,

Institute of Physical Chemistry, University of Uppsala, Box 532, 751 21 Uppsala, Sweden

Søren Hvidt,

Chemistry Department, Roskilde University and Risø National Laboratory, Roskilde, DK-4000 Denmark

and Pratap Bahadur

Department of Chemistry, South Gujarat University, Surat 395007, India *(Received: June 5, 1990)*

The properties of aqueous solutions of low molecular weight triblock copolymers of PEO/PPO/PEO have been investigated, mainly by dynamic and static light scattering. At low concentrations ($C < 10\%$) and temperature (<25 °C) the relaxation time distributions from dynamic light scattering show the coexistence of the monomer ($R_H \approx 18$ Å), micelles ($R_H \approx 80$ Å), and micellar aggregates in relative proportions which depend critically on temperature and concentration. Micelles are formed at about $C = 5\%$ at 25 °C. At 40 °C and above micelles are present at all concentrations used ($C > 0.3\%$). At infinite dilution the hydrodynamic radius of the micelles is approximately constant over the temperature range 15-50 °C. At finite concentrations the apparent micellar radius increases with increasing temperature. The growth into asymmetric particles with increasing concentration is stronger as demonstrated by ultracentrifugation and combining static and dynamic light scattering data. At higher concentrations, a solidlike gel is formed at a well-defined temperature as shown by oscillatory shear measurements. It is characterized by a dynamic correlation length which decreases monotonically with increasing concentration to about 20 Å.

Introduction

PEO/PPO/PEO block copolymers are widely used, nonionic surface-active agents.[1,2] They are low molecular weight substances known as poloxamers: the presently used material (designated Pluronics P-85) has a monomeric molecular weight of 4500, of which 50% corresponds to the PEO moiety. P-85 forms micelles in aqueous solution which, in analogy with other micelle-forming block copolymers,[3] are presumably composed of a core of the water-insoluble PPO blocks with a swollen shell of PEO end blocks. The properties of such materials in solution, such as the cloud point and their propensity to form gels, are markedly dependent on the relative sizes of the blocks and also on the overall molecular weight.

Until recently, the characteristics of these copolymers had not been reported in any detail in the literature. Zhou and Chu[3a] described "anomalous" association behavior in an analogous ABA block copolymer (L-64) having lower molecular weight. It appears, however, that this artifactual behavior is characteristic of the particular preparation. Subsequently, these authors studied the aggregation behavior of a similar copolymer (Pluronic F-68) at low concentrations using light scattering.[3b]

Our interest in this type of compound was stimulated by the observation that, after an initial rearrangement of the structure to form micelles, at higher concentrations the latter associate over a narrow temperature interval to form a rigid gel, the transition temperature depending strongly on the solution concentration. The main emphasis in this communication is placed on static and dynamic light scattering as well as dynamic mechanical measurements to examine (i) associative phenomena in the system, (ii) the micelle/gel transition, and (iii) the relaxation characteristics of the gel formed at higher temperatures/concentrations.

Relaxation time distributions have been obtained by inverse Laplace transformation (ILT) from the dynamic light scattering time correlation functions over a wide span of concentration (up to 0.38 g mL^{-1}) and temperature up to the cloud point at the particular concentration. Dynamic mechanical measurements over a broad frequency range were performed as a complement. More detailed reports of the viscoelastic properties and of a small-angle neutron scattering study on this system will be described elsewhere. Close to completion of this phase of the project, we became aware of a similar investigation[4] of some closely related copolymers, although the main emphasis there was not placed on the elucidation of the properties using light scattering techniques.

(1) *Non-ionic surfactants, Physical Chemistry*; Schick, M. J., Ed.; Marcel Dekker: New York, 1987.
(2) Tuzar, Z.; Kratochvil, P. *Adv. Colloid Interface Sci.* **1976**, *6*, 201.
(3) (a) Zhou, Z.; Chu, B. *Macromolecules* **1987**, *20*, 3091. (b) Zhou, Z.; Chu, B. *J. Colloid Interface Sci.* **1988**, *126*, 171.
(4) Wanka, G.; Hoffmann, H.; Ulbricht, W. *Colloid Polym. Sci.* **1990**, *268*, 101.

0022-3654/91/2095-1850$02.50/0

Experimental Section

The block copolymer Pluronics P-85 was obtained from Serva AG, Heidelberg, West Germany, and used without further purification. It has a declared molecular weight of 4500, 2200 for the PEO component and 2300 for PPO ($E_XP_YE_X$, where $X = 25$, $Y = 40$).

High-pressure liquid chromatography was made on the P-85 sample dissolved in tetrahydrofuran in a column that had been previously calibrated with polystyrene standards (column: 30 cm PL gel, 1000 Å; 30 cm PL gel, 500 Å; 60 cm PL gel, 10 Å). The elution rate was 1 mL min^{-1}. Since P-85 and similar materials are known to contain small contaminating quantities of the diblock copolymer, the main peak was assigned to the triblock PEO/PPO/PEO copolymer and the subsidiary peak eluting at a greater volume and making up about 10% of the material applied to the column, to the diblock PEO/PPO copolymer. As will be shown below, the diblock contaminant is evident in the experiments made at low concentrations where the monomer constitutes the dominant form but is probably absorbed into the core of the micelles formed at concentrations above about 5%.

Static Light Scattering. Intensity light scattering measurements were made using a photon-counting apparatus supplied by Hamamatsu to register the scattered signal. The light source was a 3-mW He–Ne laser. The optical constant for vertically polarized light is $K = 4\pi n_0^2(dn/dc)^2(N_A \lambda^4)$, where n_0 is the solvent refractive index, dn/dc the measured refractive index increment (=0.132 ± 0.002 mL g^{-1} at 25–50 °C), and λ is the wavelength (633 nm). The reduced scattered intensity, KC/R_θ, was derived where C is the concentration and R_θ is the Rayleigh ratio obtained through calibration using benzene; $R_{90} = 8.51 \times 10^{-6}$.[5] The angle-corrected intensity for benzene was constant over the angular range 45°–135°. The inverse osmotic compressibility was evaluated from the KC/R_θ values.

Dynamic light scattering measurements have been made using the apparatus and technique described in ref 6. Laplace inversion of the correlation curves was performed using a constrained regularization program REPES[7] to obtain the distribution of decay times. The algorithm differs in a significant respect from CONTIN[8] in that the program directly minimizes the sum of the squared differences between the experimental and calculated $g^2(t)$ functions using nonlinear programming, and the a priori chosen parameter "probability to reject" was selected as $P = 0.5$. The decay time distributions were closely similar to those obtained by using CONTIN with a similar degree of smoothing.

Distributions have been obtained as described in ref 20, by fitting to the sum of a Gaussian peak and a generalized exponential function (GEX) to describe the broad distributions of slowly relaxing components which occur in the vicinity of the gel point.

Intrinsic viscosity measurements on dilute solutions were made at various temperatures using an Ubbelohde capillary viscometer. Values are given in Table I.

Oscillatory shear viscosity measurements were made using a Rheometrics RFS 8500 instrument with a fluid bath temperature control (±0.1 °C). A cone and plate geometry cell (diameter 50 mm, angle 0.02 rad) was used for all measurements. Samples were cooled in the refrigerator (5 °C) prior to transfer to the apparatus. Storage and loss moduli, G' and G'', were measured as a function of frequency between 10^{-2} and 10^2 rad/s; 5–10 points per decade were measured. The main focus here was placed on the shear modulus as a function of temperature. A frequency of 1 rad/s was employed. The heating rate was 0.5 °C/min except in the vicinity of the gelation temperature when it was reduced to 0.1 °C/min. The strain amplitude dependence of the viscoelastic data was checked for several samples, and measurements were only performed in the linear range where moduli are independent of strain amplitude. The strain amplitude was lower during the transition, the torque being maintained at approximately 10^{-4} N m. Typical strain amplitudes were varied between 0.1% and 50%, depending on concentration and temperature.

Sedimentation measurements were made at 54 000 rpm using an MSE analytical ultracentrifuge (Centriscan 75) equipped with schlieren optics, at the temperatures 25, 40, and 50 °C over the concentration range at which micelles were shown to exist by dynamic light scattering. At 50 °C and at the highest concentrations, it was necessary to run for 20 h since the buoyancy factor was small and the sedimentation rate very slow.

Partial specific volume measurements were made using a Kratky digital densimeter (Model DMA02, A. Paar, AG, Graz, Austria). The partial specific volume, $\bar{v}_2$, was obtained as the tangent to plots of V (the volume of solution containing 1 kg of solvent) versus unitless concentration (kg of polymer per kg of

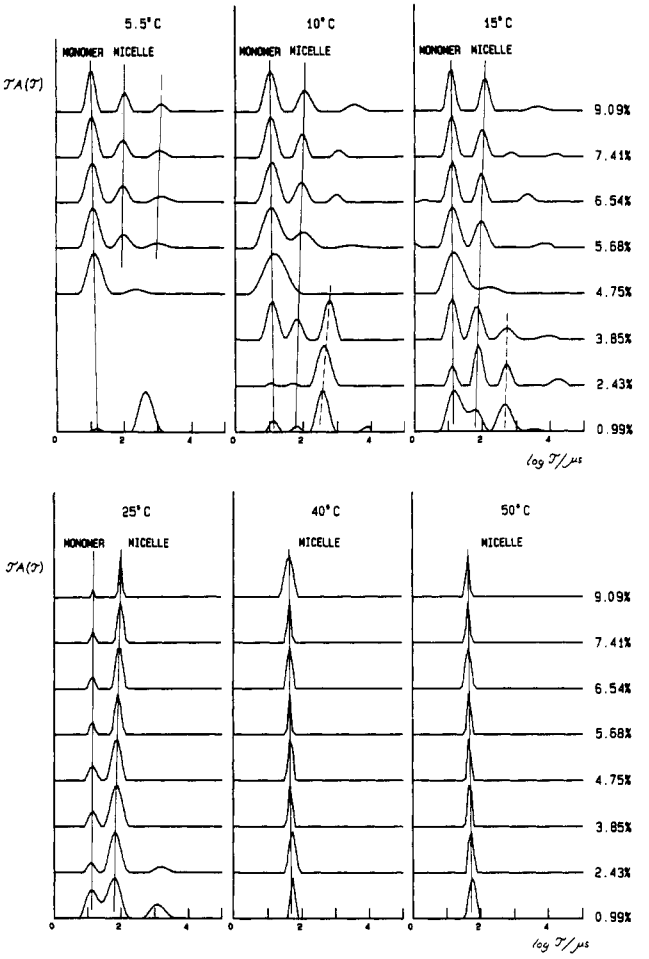

Figure 1. Relaxation time distributions obtained by Laplace inversion of dynamic light scattering data, $\tau A(\tau)$ vs log $\tau/\mu s$, for P-85 at low concentrations ($C < 10\%$) and at temperatures between 5 and 50 °C. Peaks attributed to monomer and micelles are indicated in addition to the peaks at low concentration which probably reflect clusters of diblock contaminant. Measurements are at an angle of 130°.

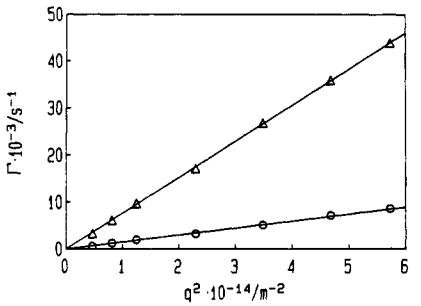

Figure 2. Plot of decay rate vs the square of the scattering vector, $\mathbf{q}^2$, for $C = 19.9\%$ at 25 °C. The fast mode is attributed to the monomer and the slow mode to the micellar component.

(5) Pike, E. R.; Pomeroy, W. R. M.; Vaughan, J. M. *J. Chem. Phys.* **1975**, *62*, 3188.
(6) Nicolai, T.; Brown, W.; Johnsen, R. M.; Štěpánek, P. *Macromolecules* **1990**, *23*, 1165.
(7) Jakeš, J. *Czech. J. Phys.* **1988**, *B38*, 1305.
(8) Provencher, S. W. *Makromol. Chem.* **1979**, *180*, 201.

TABLE I: Hydrodynamic Radii (in Å) from Dynamic Light Scattering and Pulsed Field Gradient NMR and Apparent Molecular Weights from Intensity Light Scattering

Dynamic Light Scattering

			aggregates	
T, °C	monomer	micelle	0.5% < C < 4%	6% < C < 10%
5.5	18		*a*	1720
10	18		460	2370
15	18	93	620	4660
25	18	80		
40		80		
50		80		

PFG-NMR

T, °C	micelle	T, °C	r_{equiv}[c]
21.3	62		
24.5	71	25	65
30.6	85	40	85
35.7	90	50	98

Intensity Light Scattering

T, °C	$(M_w)_{app} \times 10^{-3}$	$(n_w)_{app}$	$[\eta]$, mL g^{-1}
9.7	(90)	(20)	
14.7	(96)	(21)	16.0
25	(42)		12.6
39.9	134	30	8.6
49.8	194	43	6.5

Diffusion Coefficients and Sedimentation Coefficients at Infinite Dilution

T, °C	$D_0 \times 10^{12}$, m^2 s^{-1}	$s_0 \times 10^{13}$, s	$\bar{v}$, mL g^{-1}	$M_{s,D} \times 10^{-3}$
25	30.6	2.55	0.901	203
40	44.6	4.22	0.914[b]	264
50	53.2	5.15	0.923	308

[a] Precipitate. [b] Interpolated. [c] At gelling concentration (close packing).

solvent). The partial specific volume was independent of concentration but significantly dependent on temperature.

Differential scanning calorimetry (DSC) measurements were made on a Perkin-Elmer DSC-7 instrument using 20 μL of P-85 solution and water as the reference, in paired aluminum capsules. Scan rates were either 1 or 5 °C/min in both heating and cooling scans.

Results and Discussion

Dynamic Light Scattering: Dilute Solutions ($c < 0.1$ g/mL). Figure 1 shows relaxation time distributions in the concentration range 0.3×10^{-2} to 0.10 g/mL obtained by inverse Laplace transformation (ILT) of the autocorrelation functions at several temperatures extending up to 50 °C which approximates the cloud point at the higher concentrations.

The peaks observed are diffusive; Figure 2 shows that the relaxation rates are linearly dependent on the square of the scattering vector, q.

The relaxation time distributions for 5.5–15 °C are dominated by the monomer peak and the slower micelle peak. Even slower components are also present: below C = 5% they contribute a major part of the scattering intensity and probably represent aggregates of the diblock copolymer. The pure triblock was separated by using HPLC and shows only the monomer. Above 5%, however, the slowest component probably derives from micellar clusters. Evidence for micelle formation at $C > 5\%$ and the presence of aggregates, which are about 5 times greater in diameter, is presented below.

The distributions obtained at 25 °C show that the peak associated with the large aggregates disappears at between 2.5% and 4%, and the distributions become bimodal. Plots of the diffusion coefficients reduced by using the solvent viscosity and absolute temperature are shown in Figure 3A,B. The value at infinite dilution may be used to calculate the effective hydrodynamic radius from the Stokes–Einstein equation. There appears to be a common intercept at C = 0 in each case (with the exception of the data

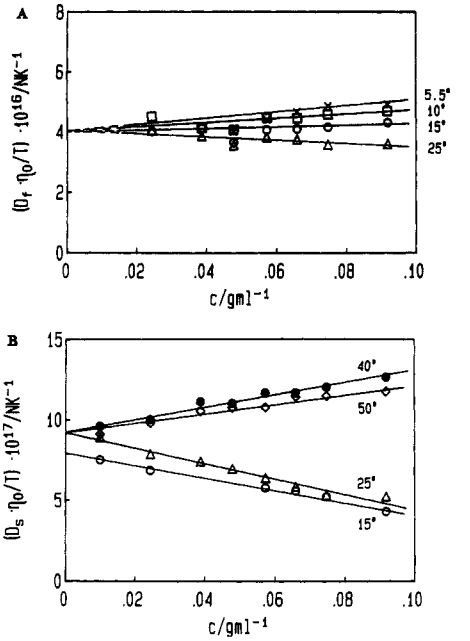

Figure 3. Plots of the reduced diffusion coefficients, using absolute temperature and solvent viscosity, for data at different temperatures and corresponding to the two modes of shortest relaxation time in Figure 1. (A) 5.5 (×), 10 (□), 15 (○), and 25 °C (△). $(R_H)_{c=0}$ = 18 Å. (B) 15 (○), 25 (△), 50 (◇), and 40 °C (●). $(R_H)_{c=0}$ = 80 Å.

for the slower mode at 15 °C), suggesting that the hydrodynamic radius is approximately constant over the range of temperature 15–50 °C; we obtain 18 and 80 Å respectively for the fast (A) and slow (B) species. The interpretation is made that these correspond to monomer and micelle, respectively (Table I). We note that Zhou and Chu[3b] and Wanka et al.[4] describe micelles of similar hydrodynamic radius. Moreover, the hydrodynamic radius remained approximately constant while the molecular weight increased owing to changes in the PEO solvation pattern.

The copolymer molecule has an average molecular weight of 4500, of which about 50% corresponds to the PEO blocks. With monomer unit weights of 44 in PEO and 58 in PPO, this means about 40 propylene oxide chain units in the central block and 25 ethylene oxide units on either side. The hard-sphere radius for a molecule of M = 4500 would be 11.5 Å. Thus, from the 18-Å radius, one may conclude that the monomer is highly compact, possibly with the PEO chains forming a tight shell about the nonhydrated PPO core.

At the lowest concentrations ($C < 5\%$) and temperatures (≈5 °C) one approaches a phase boundary, forming the solubility limit of the monomer. At 5.5 °C visible clouding is observed in the concentration range $1\% > C < 5\%$, and for this reason distributions are not given for these solutions in Figure 1. At concentrations between 0.5% and 5% and at the temperatures of 10 and 15 °C, a slow peak is also present which is at present attributed to aggregates of the small amount of the relatively hydrophobic diblock monomer which is present. Increasing concentration favors micelle formation, however, and one may surmise that the micelles progressively solubilize the minor component. Since increasing temperature also favors micelle formation, the minor component is then diminished at even lower concentrations at the higher temperatures.

Above C = 5–6%, on the other hand, monomer, micelles, and micellar clusters coexist in the temperature range 5–15 °C, the last named having a size which increases with increasing temperature. The plots of $(D\eta_0/T)$ vs C shown in Figure 4 reveal that the clusters are substantially larger above C = 5% than below this concentration (η_0 is the solvent viscosity). Approximate estimations of the aggregate sizes are given in Table I.

The distributions at 25 °C (Figure 1) are bimodal above $C \approx$ 3% (monomer plus micelle), while those at 40 and 50 °C consist of a single peak representing the micelle which is the only scat-

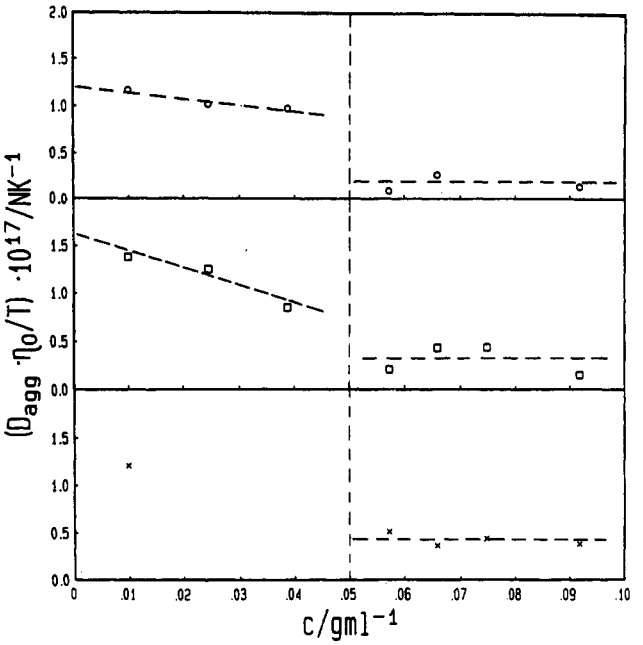

Figure 4. Plots of reduced diffusion coefficients for aggregate peaks in Figure 1: top, 15 °C; middle, 10 °C; bottom, 5.5 °C. Approximate hydrodynamic radii of the aggregates are given in Table I. At low concentrations ($C < 5\%$) the aggregates probably correspond to clusters of the diblock copolymer and at $C > 5\%$ to clusters of the micelles.

tering particle present at these temperatures in the concentration range $1\% < C < 10\%$. This shows that the critical micelle concentration (cmc) is much lower at 40 and 50 °C than at the lower temperatures.

The progressive change in the distributions with change in temperature is shown in Figure 5A for $C = 4.8\%$. A temperature/viscosity shift (η_0/T) has been made on the log time axis to facilitate comparisons. This plot emphasizes the complexity of the system in the low concentration/temperature ranges and in particular in the region just below 25 °C. The latter range is shown in more detail in Figure 5B, which reveals the strong change in the relative amplitudes of monomer/micelle contributions. One may conclude that micellization occurs gradually over a range of temperature in the vicinity of 25 °C (the critical micelle temperature, cmt) at this concentration; see also the discussion below on the concentration dependence of the inverse osmotic compressibility. Thus, $C = 5\%$ corresponds approximately to the cmc at 25 °C. Since the sizes of micelle and monomer are very different, however, the peak areas reflecting the relative intensity contributions do not give a ready indication of the numbers of the two species.

Intrinsic viscosity measurements (capillary viscometry) were made on dilute solutions in order to obtain more information on the micellar dimensions. The intrinsic viscosity decreases from 16 mL g^{-1} at 15 °C to 6.5 mL g^{-1} at 50 °C. These values are close to those which were determined by extrapolating the shear viscosity measurements to zero shear. The reduction in intrinsic viscosity at higher temperatures is anticipated since only the micellar form exists above 40 °C, whereas a complex mixture of monomers/aggregates and micelles is present at temperatures lower than 25 °C. The intrinsic viscosity is then not readily interpreted.

Assuming that the particle of $R_H = 80$ Å is a micelle, one may speculate on its structure using classical methods. The intrinsic viscosity 6.5 mL g^{-1} at 50 °C suggests a very compact particle although with some disymmetry and/or solvation. With the partial specific volume $v_2 = 0.92$ mL g^{-1} and assuming a reasonable value for the solvation of 1 g of H_2O per g of P-85 (that given in ref 9 for PEO-containing micelles), a shape factor of 3.6 is obtained. The latter corresponds to a ratio $(b/a) \approx 3.8$ for the prolate

(9) Robson, R. J.; Dennis, E. A. *J. Phys. Chem.* **1977**, *81*, 1075.

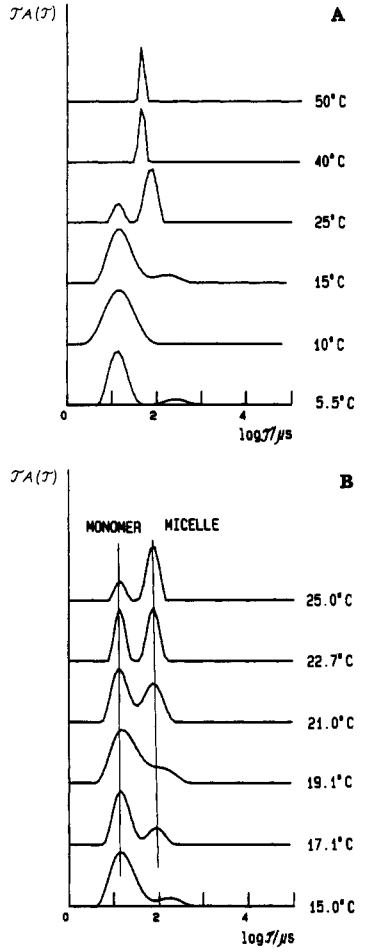

Figure 5. (A) Transition monomer:micelle. Relaxation time distributions for P-85 at $C = 4.8\%$ as a function of temperature. Measurements at angle 130°. (B) shows the interval between 15 and 25 °C.

ellipsoid, where b and a are the semimajor and semiminor axes. Introducing the value 3.8 into Broersma's relationship for the hydrodynamic radius[10] yields a rod length $L = 240$ Å. This means a radius $r = 64$ Å. The corresponding radius of gyration, R_g, is 83 Å, calculated from Broersma's equation:

$$R_g^2 = [(L^2/12) + (r^2/2)] \quad (1)$$

With reservation regarding the applicability of the Flory–Fox relationship for such compact particles and using the intrinsic viscosity at 50 °C and the value $M = 3.08 \times 10^5$ (see Table I) ($[\eta] = 2.1 \times 10^{21}(6^{3/2})(R_g^3/M)$), one obtains $R_g = 86$ Å. Values for the hydrodynamic radii of the micellar component from self-diffusion coefficients measured by pulsed-field-gradient NMR[11] and extrapolated to infinite dilution are included in Table I. These vary between 62 and 90 Å in the temperature range 21.3–35.7 °C, with an average value of 77 Å. The trend with temperature contrasts with the constant micelle radius from dynamic light scattering. This is possibly the result of polydispersity since a number-average quantity is obtained with NMR which will be very sensitive to even small amounts of monomer. Evaluation is through force fitting to a single exponential, and at the temperatures used the suspension is paucidisperse; see Figure 1. Thus, the difference between the hydrodynamic radii from PFG-NMR and DLS is less at the higher temperatures at which the suspension is nearly monodisperse.

If the micelle is a hard sphere, the radius may be estimated from

$$R = (3M_{s,D}\bar{v}_2/4\pi N_A)^{1/3} \quad (2)$$

(10) (a) Broersma, S. *J. Chem. Phys.* **1960**, *32*, 1626. (b) Imae, T.; Kamiya, R.; Ikeda, S. *J. Colloid Interface Sci.* **1985**, *108*, 215.

(11) Li, P. Personal communication (unpublished results).

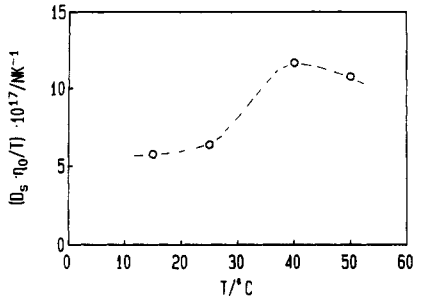

Figure 6. Reduced diffusion coefficient for the micellar mode in a solution with C = 5.7% as a function of temperature (see eq 3).

with $\bar{v}_2$ the partial specific volume. At 50 °C a value of R = 48 Å is obtained. Since experiment gives approximately double this value, one may conclude that the hard-sphere model is invalid for the micelle conformation at this temperature; see discussion below in conjunction with Figure 13.

Figure 6 shows a plot of $(D\eta_0/T)$ as a function of temperature at a concentration of 5.7%. The apparently anomalous increase in the reduced diffusion coefficient commencing at about 25 °C implies conformational changes in the ethylene oxide chains and micellar growth, since there is a simultaneous increase in the molecular weight (see Table I). We may write for the reduced mutual diffusion coefficient

$$(D\eta_0/T) = M(\partial\pi/\partial c)/6\pi N_A r_s T \qquad (3)$$

for a hard-sphere radius r_s. Since $(\partial\pi/\partial c)$ decreases strongly with increasing temperature (see Figure 14) and the radius (at infinite dilution) is approximately constant or increases (Table I), the larger values of $(D\eta_0/T)$ at 40 and 50 °C must be due to an overriding increase in the particle molecular weight with increase in temperature above 25 °C.

To some extent, a parallel may be drawn with the nonionic, poly(ethylene oxide) containing, amphiphile $C_{12}E_6$, for which the second virial coefficient becomes negative at about 21 °C and above this temperature micellar growth becomes marked.[12]

Sedimentation Results. Analytical centrifugation can provide a measure of the molecular weight through combination of the sedimentation and diffusion coefficients at infinite dilution at a given temperature. Measurements were made on the system in the temperature/concentration range where the micelle is the predominant entity. Values of the sedimentation coefficient at infinite dilution are included in Table *I* for 25, 40, and 50 °C and confirm the general picture regarding a modest growth of the micelles with increasing temperature. The complex average molecular weight, $M_{s,D}$, is consistently higher than the weight average values from static light scattering. Since the micelle is the sedimenting entity in ultracentrifugation and this quantity is combined in the Svedberg equation with the diffusion coefficient for the micellar peak in the relaxation time distribution, the values of $M_{s,D}$ are considered to be reliable molecular weights. The partial specific volume was measured by using the densimetric technique described in the Experimental Section at a series of concentrations and in the range 15–50 °C.

The sedimentation coefficient is inversely proportional to the friction coefficient. Thus, the frictional coefficient ratio, f/f_0,[22]

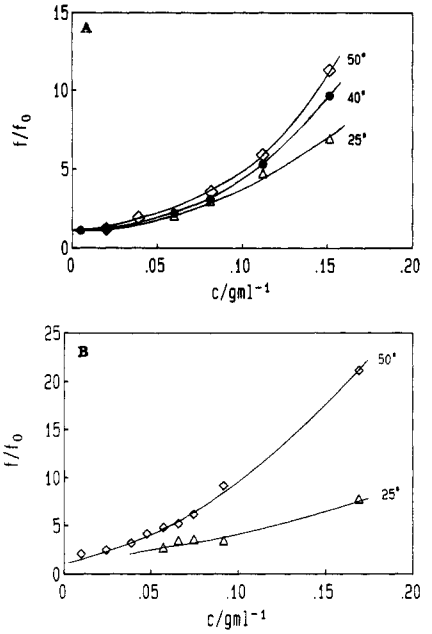

Figure 7. (A) Dependence of the frictional ratio, f/f_0, derived from the sedimentation coefficient (eq 4) for P-85 as a function of concentration at 25 (△), 40 (●), and 50 °C (◇). The trend shows the increasing asymmetry (solvation) of the micelle as a function of concentration. (B) Frictional ratio (f/f_0) evaluated via eq 5, shown as a function of P-85 concentration at the temperatures 25 (△) and 50 °C (◇).

may be estimated from the following expression (where f is the friction coefficient at a given concentration, f_0 is the value for the sphere, and $(1 - \bar{v}_2\rho)$ is the buoyancy factor with v_2 and ρ the partial specific volume and density of the solution at concentration C (superscript 0 denotes solvent):

$$f/f_0 = [(s_0/s)(1 - \bar{v}_2\rho)/(1 - v_2^\circ\rho^\circ)] \qquad (4)$$

f/f_0, which equals unity for spherical, nonhydrated particles, is shown as a function of concentration of P-85 at the three temperatures in Figure 7A. Since solvation certainly decreases with increasing temperature, it is clear that the asymmetry of the micelle increases strongly with increasing concentration in the temperature interval 25–50 °C and that the change in size of the micelles with temperature change at a given concentration is, by comparison, small. The friction coefficient may be also evaluated from the diffusion coefficient and the osmotic compressibility via the equation

$$f = (kT/D)[(M/RT)(\partial\pi/\partial c)] \qquad (5)$$

Figure 7B shows the frictional ratio (f/f_0) evaluated using eq 5 at 25 and 50 °C as a function of concentration and the pattern is similar to that in Figure 7A.

High Concentrations ($C > 10\%$). Examination of the relaxation time distributions from dynamic light scattering over a broader range of concentrations at various temperatures (Figure 8) reveals substantial changes with concentration and temperature. The distributions at, for example, 25 °C become less well-defined above about 20% and are made up of a fairly narrow Gaussian peak and a broad, slow, diffusional peak representing very polydisperse aggregates of micelles. Both components are linearly dependent on the square of the scattering vector. This characteristic pattern commences well below and continues to well above the concentration at which a solidlike gel is observed by oscillatory shear measurements at this temperature.

Finally, at the very highest concentrations, the slow part of the spectrum which is observed at low concentrations is almost completely absent. Thus, this diagram shows the progressive devel-

(12) Brown, W.; Rymdén, R. *J. Phys. Chem.* **1987**, *91*, 3565.
(13) Geissler, E.; Hecht, A. M.; Duplessix, R. *J. Polym. Sci., Polym. Phys. Ed.* **1982**, *20*, 225.
(14) Brown, W.; Mortensen, K. *Macromolecules* **1988**, *21*, 420.
(15) Brown, W.; Fang, L. *Polymer*, in press.
(16) Richtering, W. H.; Burchard, W.; Jahns, E.; Finkelmann, H. *J. Phys. Chem.* **1988**, *92*, 6032.
(17) Carnahan, N. E.; Starling, K. E. *J. Chem. Phys.* **1969**, *51*, 635.
(18) Brown, W.; Zhou, P.; Rymdén, R. *J. Phys. Chem.* **1988**, *92*, 6086.
(19) Higgins, J. S.; Blake, S.; Tomlins, P. E.; Ross-Murphy, S. B.; Staples, E.; Penfold, J.; Dawkins, J. V. *Polymer* **1988**, *29*, 1968.
(20) Nicolai, T.; Brown, W.; Hvidt, S.; Heller, K. *Macromolecules* **1990**, *23*, 5088.
(21) Brown, W.; Mortensen, K.; Pedersen, J. To be published.
(22) Svedberg, T.; Pedersen, K. O. *The Ultracentrifuge*; Oxford University Press: Oxford, 1940.

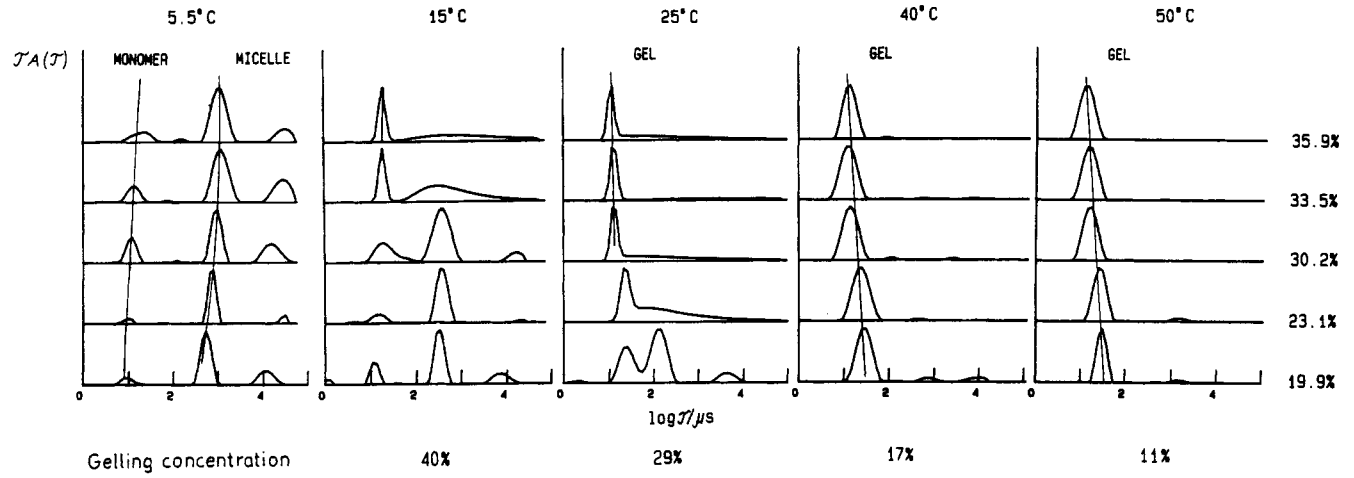

Figure 8. Relaxation time distributions for higher concentrations ($C > 10\%$) of P-85/water at the temperatures indicated. The viscoelastic gelling temperatures are 15 °C, 40%; 25 °C, 29%; 40 °C, 17%; and 50 °C, 11%.

opment from monomer to micelle, through development of the gel at intermediate concentrations, to an almost homogeneous gel at high concentration. The distributions shown in Figure 8 at 40 and 50 °C show only the single Gaussian peak describing the relaxation of the gel structure.

Two characteristic length scales are frequently used when discussing gel structure.[23] The first (ξ_H) describes the screening of hydrodynamic interactions and may be defined in terms of the cooperative diffusion coefficient measured in DLS experiments

$$\xi_H = kT/6\pi\eta_0 D \qquad (6)$$

where η_0 is the solvent viscosity and kT the energy term. It is used to characterize either the transient network formed by overlapped (entangled) chains or permanent networks formed through cross-linking. ξ_H is simply related to the distance between entanglement points for linear chains and decreases with increasing concentration according to a power law as the chains interpenetrate more extensively. Figure 9A shows the concentration dependence of ξ_H, characterizing the relaxation of the present gels at 40 and 50 °C in the concentration range in which gels are formed. ξ_H decreases smoothly to a value of approximately 20 Å. This infers that, subsequent to formation of the gel at the concentrations indicated by the arrows, there is a progressive increase in order with increasing concentration and formation of a tighter structure probably due to a continuous interpenetration of PEO segments or partial collapse of the PEO chains in the micellar mantle. The correlation length appears to approach a limiting value in the vicinity of 20 Å which, if it reflects the intercore dimension, implies considerable interpenetration. Using the procedure described by Zhou and Chu[3b] and assuming that the polypropylene core is essentially liquidlike, one may estimate the core radius to be of the magnitude of 40 Å. For a meander conformation in which the ethylene oxide chain in the mantle is twisted into an expanded helical form,[25] the ethylene oxide blocks would have a length of about 45 Å. The micellar dimension is then close to that determined experimentally. On the other hand, if the ethylene oxide chains in the mantle are assumed to be fully extended (zigzag form),[9] the overall size of the micelle would be unrealistically large.

The second length scale gives the range over which excluded-volume interactions are perceived (ξ_s) (static screening length) and determines the thermodynamic properties of the system. Figure 9B shows ξ_s estimated from the intensity light scattering data (see below), for concentrations at which the gel is formed, using the equation for the osmotic modulus (M_{os}):

$$M_{os} = 3kT/4\pi\xi_s^3 \qquad (7)$$

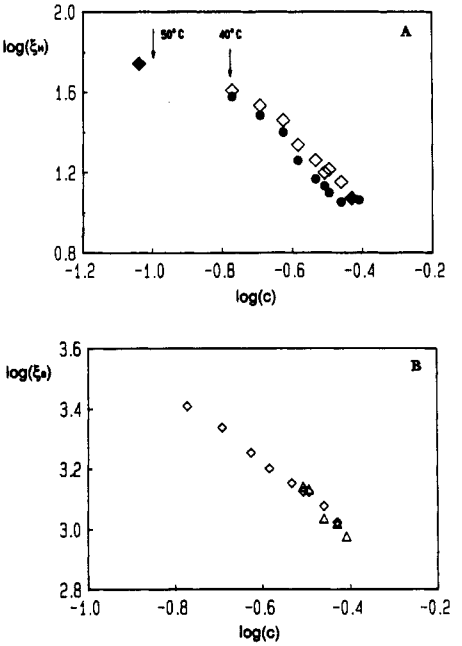

Figure 9. (A) Dependence of the dynamic correlation length (ξ_H) evaluated from eq 6 for the micellar phase at 40 (●) and 50 °C (◇). The arrows indicate the viscosimetric gelation points at the two temperatures. (B) The static correlation length (ξ_s) evaluated from intensity light scattering data using eq 7 at (△) 25 and (◇) 50 °C. The correlation lengths are given in Å and the concentrations in g mL^{-1}.

where the osmotic modulus is given by $M_{os} = C(\partial\pi/\partial c)$. This relationship was shown by Geissler et al.[13] to give values of ξ_s in agreement with experimental values from neutron scattering on poly(acrylamide) gels. With the present data, ξ_H and ξ_s differ greatly with $\xi_s \gg \xi_H$. In semidilute solutions, on the other hand, it is established that $\xi_H > \xi_s$[14] Poly(acrylamide) gels give $\xi_s \simeq \xi_H$.[15] The large values of ξ_s (of the order of 10^4 Å) found here probably reflect the presence of large voids in the gel structure.

Static Light Scattering. In order to obtain information on the apparent molecular weight $(M_w)_{app}$ and interparticle interactions, light scattering intensity (SLS) measurements were made on the same solutions used for the DLS and dynamic mechanical measurements. In addition, a series of low concentrations extending down to 0.3% were examined. The measurements always showed an insignificant dependence on angle over the range 45–135°. Plots of Kc/R_θ vs concentration are shown in Figure 10. Since single-peaked relaxation time distributions (corresponding to the micelle) only occur at 40 and 50 °C (Figure 1), an unambiguous value of $(M_w)_{app}$ (Table I) which approaches the true micellar mass can be derived only for these temperatures. In principle, the molecular weight of the micelles should be evaluated by ex-

(23) Geissler, E.; Horkay, F.; Hecht, A.-M.; Zrinyi, M. *J. Chem. Phys.* **1989**, *90*, 1924.
(24) Skoulios, A.; Tsouladze, G.; Franta, E. *J. Polym. Sci.* **1963**, *C4*, 507.
(25) Rosch, M. In *Nonionic Surfactants*; Surfactant Science Series, Vol. 1; Schick, M. J., Ed.; Marcel Dekker: New York, 1987; pp 753–793.

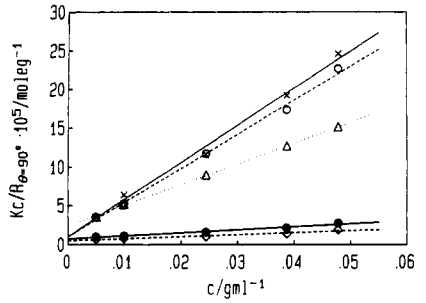

Figure 10. Reduced scattering function for P-85 in water at different temperatures: 10 (×), 15 (○), 25 (△), 40 (●), and 50 °C (◇). Molecular weights are listed in Table I.

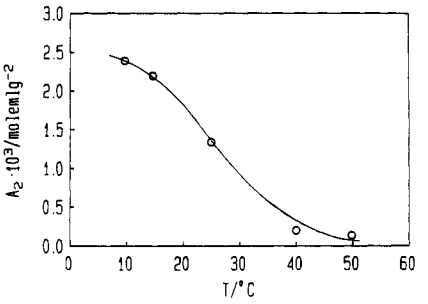

Figure 11. Second virial coefficient (A_2) as a function of temperature.

trapolation of KC/R_θ to the cmc, but at 40 and 50 °C it is not necessary to correct the concentrations for the cmc since it is insignificantly small. Micellar information cannot be meaningfully evaluated at the lower temperatures. The low value of $(M_w)_{app}$ indicated at 25 °C, for example, follows from the presence of a significant amount of the monomeric copolymer at this temperature, while at 15 and 10 °C the additional presence of micellar clusters gives a high average value of $(M_w)_{app}$.

The temperature dependence of the apparent second virial coefficient is shown in Figure 11. At 40 °C and above attractive forces become increasingly important and start to dominate over the repulsive excluded-volume forces. As is shown above (Figure 1), micelles exist at these temperatures above $C = 5\%$. At 25 °C, the equilibrium between monomer and micelle is shifted progressively in favor of micelles as the concentration is increased.

The second virial coefficient can be expressed in terms of the equivalent radius by using the expression given by Richtering et al.[16]

$$A_2 = 4V_{eq}N_A/(M_w)^2 \tag{8}$$

where $V_{eq} = (4\pi/3)r_{eq}^3$. The values of r_{eq} estimated in this way using the appropriate micellar molecular weights (Table I) are respectively 80 Å (50 °C) and 72 Å (40 °C), which agree well with the hydrodynamic radius for the micelle calculated from the diffusion coefficients at infinite dilution. In the present case A_2 is an ambiguous quantity, however, since the particle size/asymmetry changes with concentration. Nevertheless, the agreement supports the general self-consistency of the data at the higher temperatures at which micelles are the dominant species. At a given concentration, there is a pronounced growth in the micelle size with increasing temperature. Figure 12 shows the static intensity, I_{90}, as a function of temperature for $C = 4.8\%$. The rapid increase in the vicinity of 25 °C is consistent with the onset of micelle formation.

Figure 13 shows the scattered intensity as a function of concentration at two temperatures, where the intensities have been adjusted to facilitate comparison with the calculated curve for the hard-sphere model.[17] The data at 25 °C agree well with the hard-sphere model at the lower concentrations at which the intensity increases approximately linearly with C (where the positions of the scatterers are uncorrelated and the intensities additive). At 50 °C, however, the maximum of the curve is strongly displaced to lower C, which is the result expected for more asymmetrical

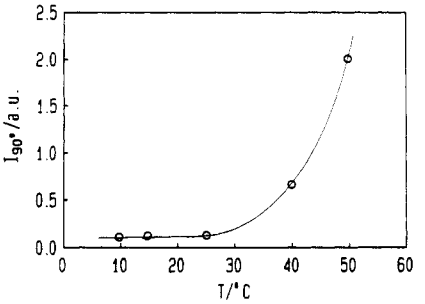

Figure 12. Plot of the intensity of scattered light (arbitrary units) as a function of temperature for P-85 in water at 4.8%.

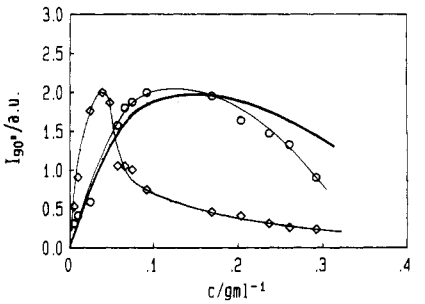

Figure 13. Intensity of scattered light (arbitrary units) as a function of concentration at 25 (○) and 50 °C (◇). The heavy line shows the theoretical intensity profile for a hard sphere taken from the equation of Carnahan and Starling.[17]

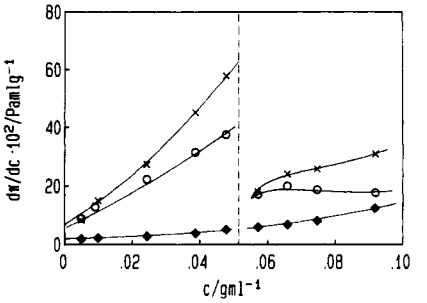

Figure 14. Inverse osmotic compressibility $(\partial\pi/\partial c)_{T,P}$ as a function of concentration in the low concentration ($C < 10\%$) range: 10 (×), 25 (○), and 50 °C (◆). The discontinuity at about 5% at 10 and 25 °C is associated with micelle formation.

particles. These observations thus also demonstrate micellar growth and increasing asymmetry with increasing temperature. Similar temperature-dependent growth was established earlier for $C_{12}E_6$ in aqueous solution.[12] The inverse osmotic compressibility was evaluated from the absolute scattered intensity at zero angle as

$$(\partial\pi/\partial c)_{T,P} = (Kc/R_\theta)_{\theta=0}RT \tag{9}$$

In dilute solution, the virial expansion has the form

$$(\partial\pi/\partial c)_{T,P} = RT/M(1 + 2A_2c + ...) \tag{10}$$

where A_2 is the second virial coefficient. The inverse osmotic compressibility is shown in Figure 14 as a function of concentration at various temperatures and shows interesting trends. In the low concentration range ($c < 5\%$), $(\partial\pi/\partial c)$ increases strongly and almost linearly with concentration for the lower temperatures of 10 and 25 °C. Here the interactions are of the type found for most water-soluble polymers and for other nonionic amphiphiles, for which the virial terms are larger at lower temperature. $(\partial\pi/\partial c)$ decreases abruptly at about 5% and then increases again in the high concentration range (Figure 15). As concluded above, the change in the vicinity of 5% is attributed to formation of the micellar phase and accompanying micellar aggregates as was shown in Figure 4. Thus, we conclude that the cmc lies close to $C = 5\%$ at 23 °C (see Figure 5B).

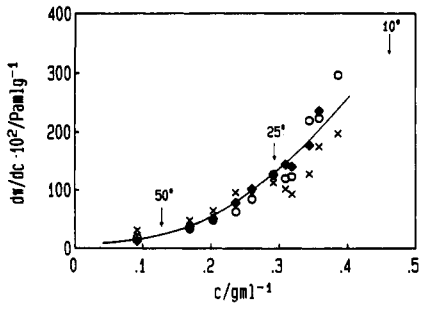

Figure 15. Concentration dependence of the inverse osmotic compressibility for the high ($C > 10\%$) concentration range: 10 (×), 25 (○), and 50 °C (◆). The arrows indicate the concentrations at which gelation is observed viscosimetrically at the three temperatures.

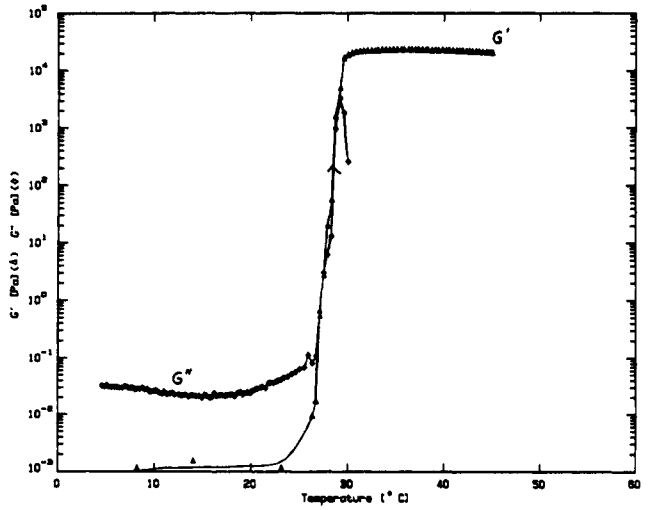

Figure 16. Storage and loss moduli, G' and G'', from oscillatory shear measurements on a P-85 solution of $C = 0.26$ g mL^{-1} at a frequency of $\omega = 1$ rad/s as a function of temperature.

It was deduced from the sedimentation data that there is a strong growth in micelle size with change in concentration. It has earlier been established that nonionic surfactants of the generic type C_xE_n in aqueous solution (where n is the number of ethylene oxide moieties) are either constant in size or grow with increasing temperature.[1]18 It is more unusual that pronounced micellar growth occurs with increasing concentration.

Above $c = 10\%$, $(\partial\pi/\partial c)$ increases monotonically with concentration (Figure 15). The data scatter significantly, owing to the difficulty in preparing optically clear solutions/gels at the highest concentrations. The progressive steric interaction between the micelles to form the precursor to the gel is not reflected in $(\partial\pi/\partial c)$, and the latter parameter has approximately the same magnitude at 10 °C (at which temperature gel is not formed at any concentration) and 50 °C (at which gel is present at all concentrations above about 10%).

Formation of Gel. At high concentrations and temperatures there is a sharp transition to a solidlike phase. Oscillatory shear viscosity measurements were made on the solutions as a function of temperature and concentration. Typical data for the elastic storage and loss shear moduli, G' and G'', are shown as a function of temperature in Figure 16. G' is small (at this concentration up to about 20 °C) followed by a strong change over a narrow interval in temperature and marking a transition from a Newtonian liquid to a solidlike gel. G'' shows an initial decrease (agreeing with the decrease in the intrinsic viscosity with increasing temperature (Table I)) followed by an increase consistent with micellar growth prior to the liquid–gel transition. Similar observations have been made by Wanka et al.[4]

The temperature–concentration curve defining the solution–gel transition derived from the oscillatory shear measurements as a function of temperature is shown in Figure 17. Here the temperature at which gelation occurs is defined as the temperature

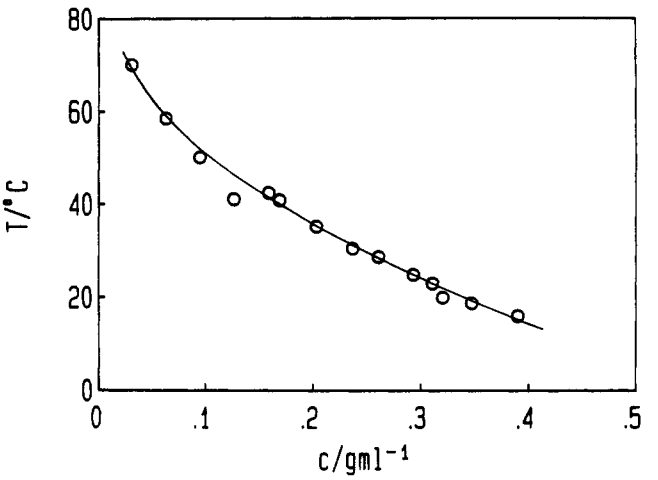

Figure 17. Gelation temperature determined from oscillatory shear measurements (the temperature at which $G' = G''$ from diagrams as in Figure 16) as a function of P-85 concentration.

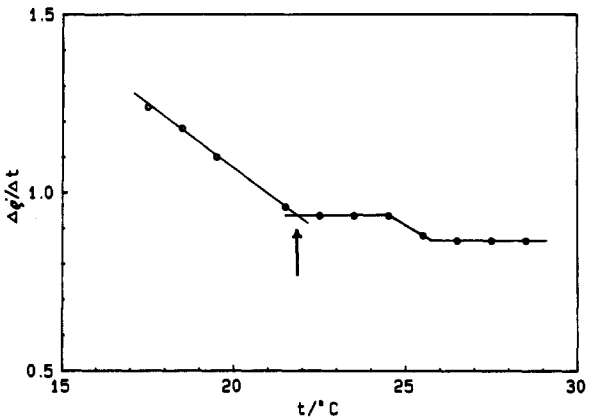

Figure 18. Plot of the density increment $(\Delta\rho'/\Delta t)$ as a function of temperature for a $C = 0.31$ g mL^{-1} P-85 solution. The viscosimetric gelation temperature is indicated by the vertical arrow.

at which G' equals G''. It was established that the gelation process is thermoreversible to within less than 1 °C, and the transition is sharp especially at the highest concentrations. G' maintains a plateau value at the highest temperatures, and the value of the plateau is greater the larger the concentration. However, measurements were, on some concentrations, carried out to the vicinity of the cloud point. At some 7–8 °C below the cloud point, G' decreased by 1–2 orders of magnitude, leveling off and becoming constant at this new value. The data suggest differences in the gel at low and high concentrations. At high concentrations and intermediate temperatures, G'' is virtually zero, while gels formed at lower concentrations and at relatively higher temperatures have significant G'' values and thus strictly speaking may be viscoelastic liquids.

Details of the viscoelastic measurements on this system will be presented elsewhere.

Gel formation is dramatic in the system. It was of interest to examine possible volumetric changes accompanying this transition. Figure 18 shows the temperature dependence of the density increment $\Delta\rho'/\Delta t$, where the latter quantity was taken between each pair of consecutive measurement points on a curve of density (ρ') vs temperature (t). The first inflection coincides precisely with the viscoelastically measured transition. The origin of the second inflection is unknown but may be related to the homogeneity of the gel or a structural rearrangement.

Assuming that gelation occurs by close packing of the micelles,[4] one may estimate the equivalent micellar radius at the concentration at which gelation is observed viscosimetrically. Using the values of $M_{s,D}$ in Table I, we find $r_{equiv} = 65$ Å (25 °C), 85 Å (40 °C), and 98 Å (50 °C). These values are consistent with those previously estimated and also show micellar growth with increasing

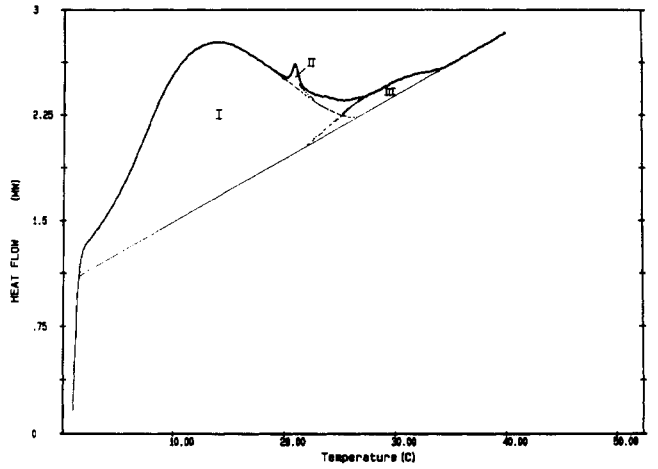

Figure 19. Differential scanning calorimetry (DSC) on a solution of P-85 at a concentration 0.326 g mL^{-1} and at a scan rate of 5 °C/min. ΔH is calculated from the area between the measured heat-rate curve and the base line. Three transitions (I–III) are discussed in the text. The viscosimetric gelation temperature coincides with peak II.

temperature. We note that Skoulios et al.[24] have earlier described this type of copolymer and the formation of lamellar structures and that they are also capable of forming liquid crystalline mesophases.

Differential scanning calorimetry measurements were made at two concentrations (28.5% and 31.1%), giving similar results. A typical thermogram is shown in Figure 19. Three processes (I–III) are indicated. Transition I contributes nearly all of the total enthalpy change of 40 ± 10 J/g and is seen as an endothermic transition in the cooling cycle. It is believed to result from monomer–micelle transitions. Transition II occurs at the gelation temperature observed in mechanical measurements (Figure 19), and ΔH is at most 2 J/g of P-85. Transition III was less reproducible and in some scans was not seen in the cooling cycle. It is possibly related to reorganization of the micelles in the gel state.

Conclusions

Triblock copolymers (PEO/PPO/PEO) exist in complex states of aggregation in aqueous solution, depending on the relative block sizes. For a particular structure, the aggregation forms are very sensitive to concentration and temperature, a feature which is characteristic of other ethylene oxide containing nonionic surfactants. Laplace inversion of dynamic light scattering data provides a novel means to elucidate the interelationships between these various aggregation states. At low concentration ($C < 10\%$) micelles form at about $C = 5\%$ at 25 °C, at which they coexist with the monomer. At 40 and 50 °C micelles form the sole scattering species and have a hydrodynamic radius of about 80 Å.

At lower temperatures, monomers, micelles, and micellar aggregates are present in proportions that depend on the concentration.

At higher concentrations, solidlike gels are formed through close packing of the micelles at well-defined temperatures (the viscoelastic gelling temperature). The characteristics of the gels and the micelle/gel transition are currently the subject of detailed investigation using SANS and oscillatory shear measurements.

Acknowledgment. The authors are indebted to Dr. Puyong Li (Stockholm) for providing NMR data, to Dr. Jesper Kristiansen (Copenhagen) for help with the DSC measurements, and to Dr. Walther Batsberg (Risø) for the high-pressure liquid chromatography determinations. We acknowledge financial support from the Swedish Natural Science Research Council and the Danish Technical Research Council.

Registry No. Pluronics P-85, 106392-12-5.

Redox and Structural Properties of Quinone-Functionalized Phosphatidylcholine Liposomes

Min D. Liu, Dale H. Patterson, Claude R. Jones,[1] and Charles R. Leidner*

Department of Chemistry, Purdue University, West Lafayette, Indiana 47906 *(Received: August 1, 1990)*

Quinone-functionalized liposomes can be prepared by the sonic dispersion of a phosphatidylcholine anthraquinone (DPPC-AQ) with simple phospholipids such as DPPC (at 52 °C) and DOPC (at room temperature). These small (ca. 25–30-nm diameter), unilamellar liposomes typically contain 4–12 mol % phospholipid quinone, which can be reduced and reoxidized by solution reagents. $S_2O_4^{2-}$ rapidly and completely reduces the liposome-bound quinones to the hydroquinone form; $Fe(CN)_6^{3-}$ rapidly reoxidizes the hydroquinone. BH_4^- reduces only those quinones situated on the outer surface of the liposome. The rates of redox reactions of the liposome-bound quinones depend on temperature and solution reactant but not on mol % DPPC-AQ in the liposomes or the quinone concentration. The rate law for $S_2O_4^{2-}$ reduction of DPPC-AQ/DOPC, $k_{obs} = k_1k_2[S_2O_4^{2-}]/(k_{-1} + k_2[S_2O_4^{2-}])$, indicates the presence of two kinetically distinct forms of DPPC-AQ. Comparison with the corresponding homogeneous rate constant suggests the identities of the two forms. Manipulation of the transmembrane, distribution of DPPC-AQ (72–98% Q_{outer}) is demonstrated by using various phospholipid compositions. Liposomes prepared from the anthracene-functionalized phospholipid DPPC-AN provide a measure of the permeability of the functionalized liposomes. ^1H NMR spectroscopy (500-MHz) reveals the structure and composition of the quinone-functionalized DPPC liposomes. Nuclear Overhauser experiments reveal that the anthraquinone "head group" of DPPC-AQ in DPPC liposomes resides near the hydrophobic–hydrophilic interface and does not extend into solution. Assimilation of these various results leads to a simple, consistent description of these novel biomimetic systems. Applicability of these and related systems as simple, chemical models for respiratory and photosynthetic energy transduction is discussed.

The phospholipid bilayer that comprises biological membranes[2] is an attractive target for biophysical and biomimetic studies. The ease with which liposomes (closed bilayer membranes) can be prepared has aided significantly in these endeavors. Numerous chemical and physical studies[4] of liposomes have revealed their

(1) Present address: Mail Zone U3E, Monsanto Agricultural Co., 800 N. Lindbergh Blvd., St. Louis, MO 63167.

(2) (a) Fendler, J. H. *Membrane Mimetic Chemistry*; Wiley: New York, 1982. (b) Harrison, R.; Lunt, G. G. *Biological Membranes*; Wiley: New York, 1980. (c) Lichtenberg, V.; Barenholz, Y. *Methods Biochem. Anal.* **1987**, *33*, 337.

0022-3654/91/2095-1858$02.50/0